European Heart Journal – Cardiovascular Imaging (2015) **16**, 198–209
doi:10.1093/ehjci/jeu179

Impact of respiration on stroke volumes in paediatric controls and in patients after Fontan procedure assessed by MR real-time phase-velocity mapping

Hermann Körperich[1]*, Peter Barth[1], Jürgen Gieseke[2], Katja Müller[3], Wolfgang Burchert[1], Hermann Esdorn[1], Deniz Kececioglu[3], Philipp Beerbaum[4], and Kai Thorsten Laser[3]

[1]Institute for Radiology, Nuclear Medicine and Molecular Imaging, Heart and Diabetes Center Northrhine-Westfalia, Ruhr-University of Bochum, Georgstraße 11, D-32545 Bad Oeynhausen, Germany; [2]Philips Healthcare, Hamburg, Germany; [3]Center for Congenital Heart Defects, Heart and Diabetes Centre Northrhine-Westfalia, Ruhr-University of Bochum, Bad Oeynhausen, Germany; and [4]Medizinische Hochschule Hannover, Kinderheilkunde, Pädiatrische Kardiologie und Pädiatrische Intensivmedizin, Hannover, Germany

Received 25 March 2014; accepted after revision 18 August 2014; online publish-ahead-of-print 22 September 2014

Aims Blood flow rate quantification using two-dimensional phase-contrast MRI (PC-MRI) results in averaging of flow information due to long acquisition times precluding the examination of short-term effects. The aim of this study was to determine respiration-related flow rate variations by non-electrocardiographic triggered real-time phase-contrast MRI (PC-MRI).

Methods and results Real-time PC-MRI was applied to study respiration-driven blood flow fluctuations in the ascending aorta (AAo), superior vena cava (SVC), and inferior vena cava (IVC) under normal and forced breathing in 33 healthy children and 10 Fontan patients. Respiration-dependent flow rates were virtually generated by dividing the respiration curve into four segments: expiration, end-expiration, inspiration, and end-inspiration. Whereas in volunteers aortic flow rate was elevated during end-expiration ($5.6 \pm 3.0\%$) and decreased during end-inspiration ($-5.8 \pm 3.5\%$) in relation to mean blood flow ($P < 0.05$), highest flow was detected during inspiration in SVC ($10.5 \pm 14.1\%$) and IVC ($22.5 \pm 12.1\%$) and lowest flow during expiration ($-11.6 \pm 13.5\%$, $-13.2 \pm 14.1\%$, $P < 0.05$). Differences were increased under forced breathing in AAo ($10.4 \pm 5.5\%$, $-7.4 \pm 6.5\%$, $P < 0.05$) and SVC ($40.0 \pm 30.3\%$, $-30.0 \pm 19.2\%$, $P < 0.05$), whereas were unchanged in IVC ($16.5 \pm 23.6\%$, $-13.7 \pm 21.6\%$, $P =$ n.s.). Regarding patients, respiratory-dependent flow rate variability was increased and had to be related to the patient's individual quality of Fontan circulation.

Conclusion Real-time PC-MRI allows a physiological assessment of respiratory-related flow rate fluctuations in healthy subjects as well as in Fontan patients. Its capability for detection of short-term effects in clinical routine was demonstrated.

Keywords MRI • Stroke volume • Respiration-dependency • Phase-velocity mapping • Pediatrics

Introduction

Velocity-encoded phase-contrast MRI (PC-MRI) is regarded as the first line diagnostic imaging technique for blood flow quantification in congenital and acquired heart disease.[1,2] Typically, conventional free-breathing two-dimensional flow measurements are performed. Due to long data acquisition times, averaging of flow information and underestimation of peak velocities occur.[3,4] Implementation of acceleration techniques for speeding up PC-MRI enables data collection in several seconds and, thus, allows measurements within a single breath-hold.[3,5,6] On the contrary, it is well-known that physiological changes during breath-holding influence haemodynamics. This results in an impaired measurement accuracy which prevents reliable diagnosis.[1,3,7,8] With the introduction of navigator techniques, the influence of respiration on blood flow measurement is compensated but is restricted to a single user-defined respiration phase.[9]

* Corresponding author. Tel: +49 5731 97 3501; Fax: +49 5731 97 1862, Email: hkoerperich@hdz-nrw.de

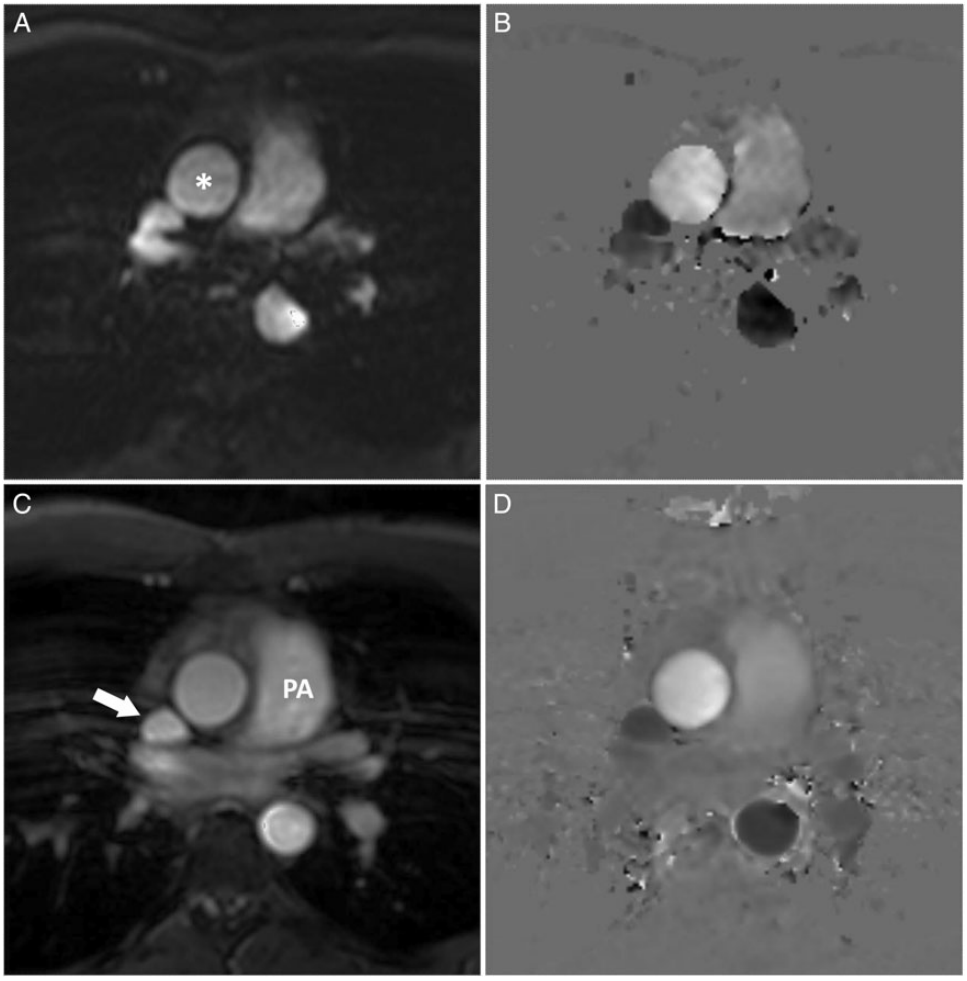

Figure 1: Phase-contrast velocity mapping. Systolic magnitude image (*A*) and the corresponding phase-contrast velocity map (*B*) obtained by non-ECG-triggered real-time PC-MRI under free-breathing condition (temporal resolution = 24 ms, male, 18.8 years). (*C*, *D*) Conventional PC-MRI. PA, pulmonary artery; arrow, superior vena cava; asterisk, ascending aorta.

In recent years, several attempts were undertaken to overcome these limitations. For this purpose, real-time PC-MRI was introduced to assess short-term effects on blood flow without any need for breath-holding.[10–14]

It is generally known that blood circulation is maintained by complex relationships between several physiological pumping systems. At least three systems with a noteworthy impact on haemodynamics should be mentioned: cardiac pump, peripheral pump which is activated by exercise, and the ventilatory pump affecting flow by intrathoracic pressure changes.[15] Especially, the passive systemic venous return through the pulmonary system in patients with functionally univentricular hearts not suitable for corrective surgery is known to be dependent on respiration after a Fontan-type operation influencing cardiac output at rest and under exercise.[16–18] Many studies carried out under physical stress are not capable to distinguish contributions based on the ventilatory pump from other influences such as the peripheral pump although exclusive modifications of the subject's breathing pattern may be helpful to investigate the quality of Fontan circulation under normal physiological conditions.

Thus, the aim of this study was to examine flow rate changes in the ascending aorta and in both caval veins in relation to different respiratory intervals occurring during normal and forced breathing in healthy volunteers by using real-time PC-MRI. In a second step, the same experimental setup is applied to Fontan patients to validate the usefulness of this method in clinical routine work. In this context, we hypothesize that the generation of virtual respiratory-gated SV curves allows a more accurate study of the ventilator system on blood flow changes.

Methods

Study design

From June 2011 to November 2012, we prospectively enrolled 34 healthy subjects without any evidence of cardiovascular diseases by echocardiography. One boy was excluded because of inability to cooperate. Of the remaining 33 participants, mean age was 13.4 ± 3.7 years (6.0–20.1 years, median = 14.1 years, 15 males). In the same period of time, 10 Fontan patients (one female) were included; mean age of 15.5 ± 3.7

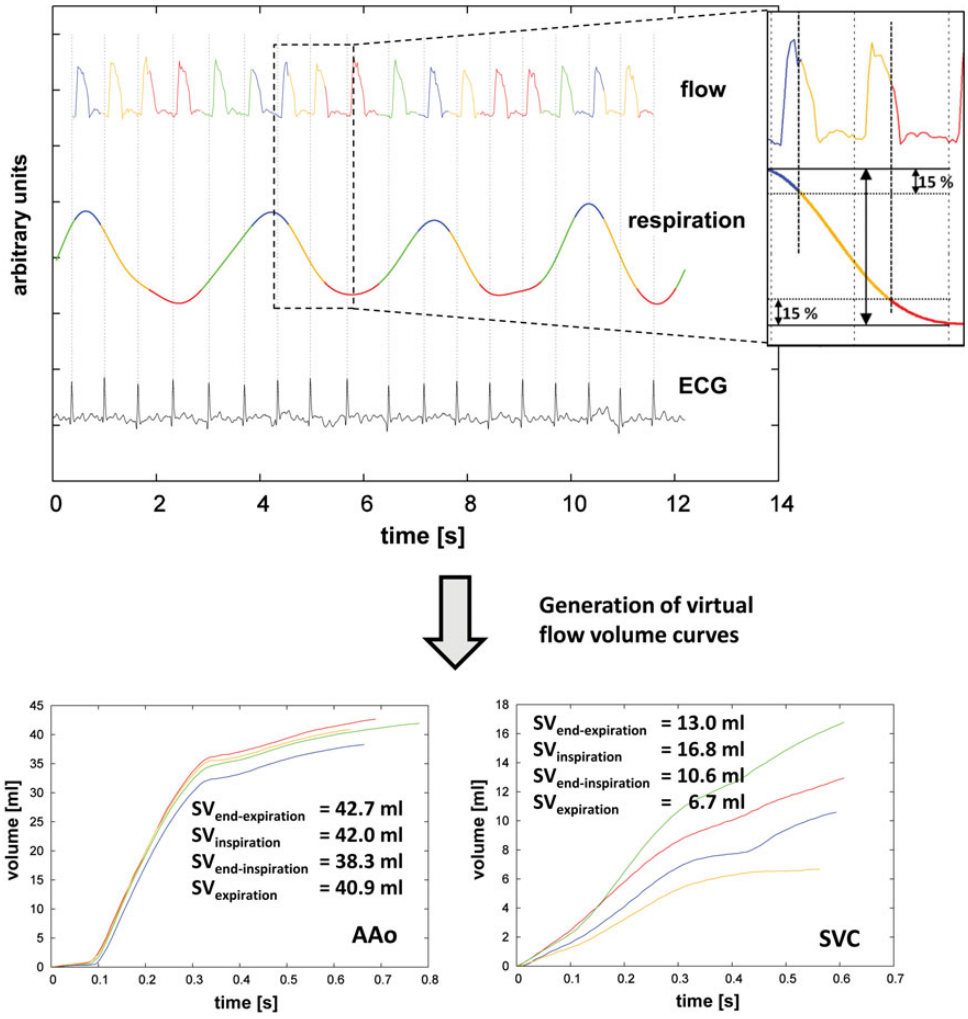

Figure 2: Generation of virtual SV curves. (Top) Division of the subject's respiration curve into four gates (red, end-expiration; green, inspiration; blue, end-inspiration; yellow, expiration). As seen in the small picture detail, occasionally heart intervals belong to different respiratory gates. The generation of respiratory-driven virtual SV curves (bottom: AAo = ascending aorta; SVC = superior vena cava) was achieved by accordingly assigning the flow data to the appropriate respiration gates. Data from a 7.9-year-old female (for the sake of clarity only physiological data from the real-time PC-MRI measurement performed in the AAo were shown).

years (11.1–22.5 years, median = 14.2 years). The study was approved by the local Scientific Ethics Institutional Review Committee (RegNo. 09/2011) and informed, written consent was obtained from study participants or legal guardians in case of minority.

After ruling out contraindications and explanation of the intended investigation, each subject underwent quantitative through-plane real-time PC-MRI measurements in the ascending aorta (AAo), superior vena cava (SVC; located prior confluence with the right atrium in controls and prior confluence with the right pulmonary artery in patients) and inferior vena cava (IVC; measuring position above hepatic veins). All flow measurements were performed under normal breathing conditions. In a second series, participants were asked to breathe in and out deeply during real-time PC-MRI data collection to investigate the amplifying respiratory impact on stroke volumes (SVs). The respiratory amplitudes were simultaneously recorded by spirometry to assess pulmonary volumes (BlueCherry Spirostik, Geratherm Respiratory GmbH, Bad Kissingen, Germany).

The quality of Fontan circulation was classified by accordingly assigning functional parameters with a possible impact on haemodynamics to define a patient-specific risk profile. In this regard, 13 parameters were assessed in every patient assigning one point for each of the following risk factors: fenestration, dilatation of the tunnel, protein loosing enteropathy, high central venous pressure (>15 mmHg), decreased oxygen saturation (<90%), significant collateral flow, diaphragmal paresis, decreased exercise capacity (peak oxygen uptake <50% of normal), bad cooperation, morphologically right systemic ventricle, significant atrioventricular valve insufficiency, reduced ejection fraction (<50%), and cardiac index (≤2.5 L/min/m^2). The following definition was applied; patient with a good Fontan circulation: risk factor between 0 and 3, moderate Fontan circulation: risk factor between 4 and 5, and bad Fontan circulation: risk factor ≥6.

For assessment of intraobserver variability, 12 randomly selected data sets (four samples of each vessel) were reevaluated by one observer;

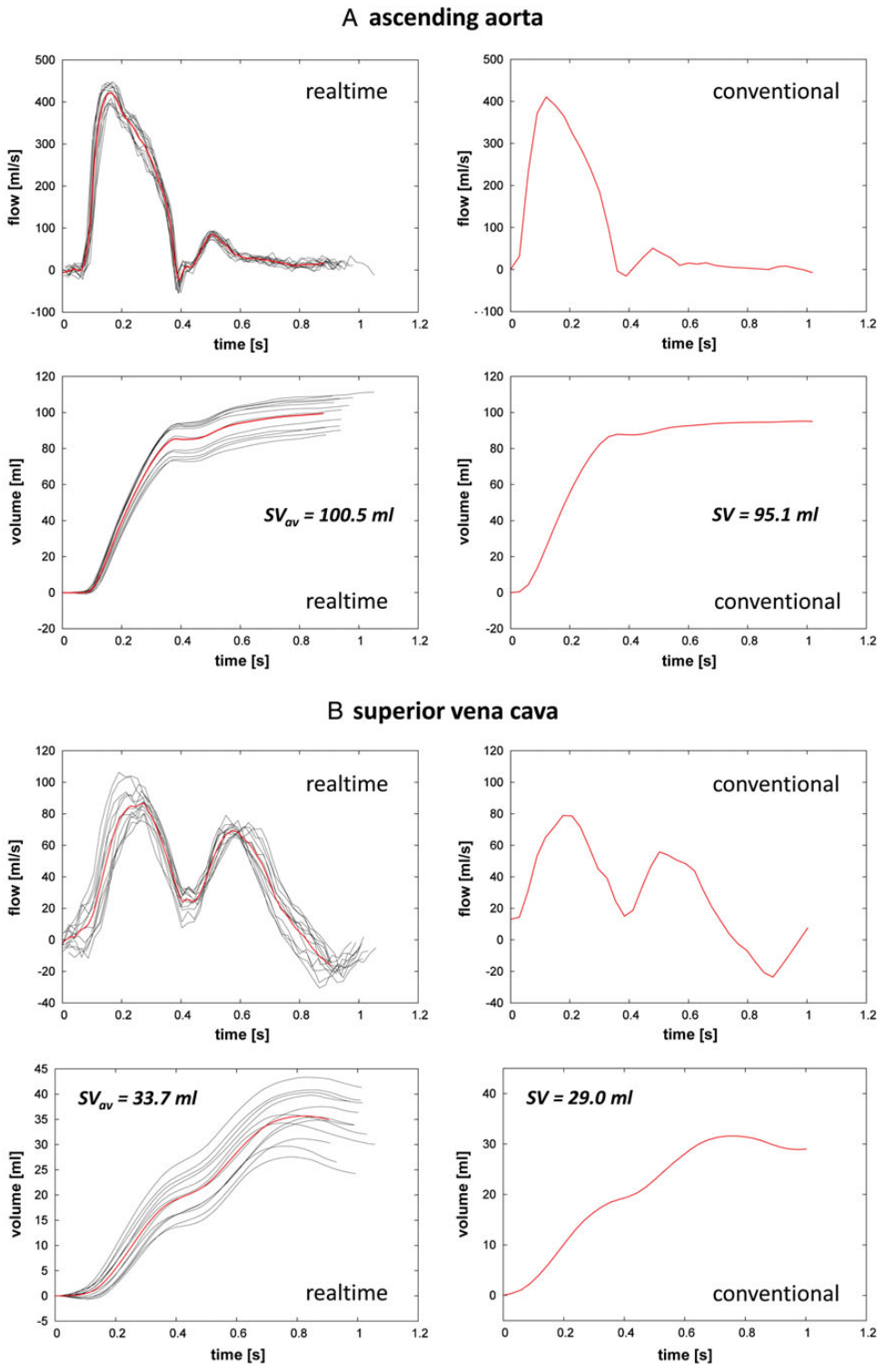

Figure 3: Flow and SV curves: real-time vs. conventional PC-MRI. (*A*) Blood flow and SV curves gathered by real-time PC-MRI during a 12 s acquisition period (female, 13.9 years, 12 heartbeats) in the ascending aorta. For comparative purposes, red line represents the average over all heartbeats. (Right column) Corresponding flow and SV curves as obtained by conventional PC-MRI (acquisition time = 1.5 min). (*B*) Accordingly, flow and SV curves in the superior vena cava. The broad variability demonstrates strong dependency from the patient's respiration.

interobserver variability was determined by two independent observers with results blinded to each other.

Magnetic resonance imaging

Quantitative flow measurements were performed with a 3.0T-TX system (Achieva, Philips Healthcare, Best, The Netherlands) equipped with parallel radiofrequency signal transmission technology (maximum gradient performance = 80 mT/m, slew rate = 200 T/m/s). A 32-element phased-array coil was used for signal detection. For vessel localization, multiple segmented multi-phase steady-state free-precession acquisitions (TR/TE/flip = 2.7 ms/1.35 ms/40°) were collected to ensure accurate through-plane PC-MRI.

Real-time PC-MRI

Real-time PC-MRI was performed using a non-ECG-triggered flow-sensitive EPI sequence combined with parallel imaging and half-Fourier technique as described elsewhere.[13,19] Spatial resolution was 2.7 × 2.7 × 6 mm^3, TR/TE_{eff} /flip = 12–14 ms/3.3 ms/40°, velocity encoding = 200 cm/s (AAo) and 100 cm/s (veins), SENSE-reduction factor = 4. With this setup, a temporal resolution of 24–28 ms was achieved (*Figure 1*). To ensure coverage of multiple breathing cycles, real-time PC-MRI was performed during a 12–14 s period resulting in 500 flow-sensitive images. Simultaneously, the subject's physiological data (ECG and respiration) as obtained by the scanner's wireless physiology units and marker information (e.g. start scan marker; stop scan marker) which is attached with the sample time moment during scanning were recorded. The facility for recording physiological data and marker information for offline evaluation purposes was provided by the manufacturer.

Table 1 Relative stroke volume variation during real-time PC-MRI depending on the subject's breathing pattern

	Stroke volume variation		*P*-value
	Normal (%)	Forced (%)	
Volunteers			
AAo	6.1 ± 1.8 (*n* = 32)	9.5 ± 3.5 (*n* = 12)	<0.05
SVC	15.8 ± 9.5 (*n* = 33)	34.8 ± 19.6 (*n* = 12)	<0.05
IVC	21.7 ± 4.7 (*n* = 10)	34.2 ± 10.2 (*n* = 9)	<0.05
Fontan pts			
AAo	10.8 ± 4.6 (*n* = 10)	11.7 ± 6.5 (*n* = 8)	—[a]
SVC	29.5 ± 17.2 (*n* = 10)	57.9 ± 46.9 (*n* = 9)	—[a]
IVC	73.0 ± 30.8 (*n* = 10)	121.1 ± 71.1 (*n* = 8)	—[a]

Mean values ± standard deviation in percent; *n* = number of data sets.
[a]No statistical analysis.

Analysis and generation of virtual SV curves

Post-processing was performed using homemade flow quantification software (developed by P.B.). Briefly, correct assignment of real-time flow data and the separately but simultaneously registered physiological data was achieved by read-out of the according timestamps for initializing and stopping of the applied pulse sequence. These flags were related to the corresponding generation time (DICOM information) of the recorded flow images.

After automatic R-wave detection, a low pass filter was applied to the respiration curve to suppress higher frequency components (>1 Hz) induced by gradient switching. Subsequently, the respiration curve was divided into four respiration sections namely: expiration, end-expiration, inspiration, and end-inspiration (*Figure 2*). The end-expiration interval was defined as the lower 15% of the difference of two adjacent maximum and minimum values, whereas the end-inspiration interval corresponds to the upper 15%.

In addition to the common representation of single flow profiles (*Figure 3*), the software allows a virtual generation and evaluation of breathing-dependent SVs as shown in *Figure 2*. Thus, flow information allocating to the same respiratory phase but although belonging to different heart cycles (picture detail, *Figure 2*) were summarized to reconstruct the new breathing-dependent flow curves allowing an accurate assignment of the subject's respiration to SVs.

Furthermore, the maximal respiratory-related indexed cardiac output difference (ΔCI_{max}) was defined as the difference between the maximal and minimal flow rates indexed to the body surface area to ensure comparability between subjects.

Statistical analysis

Statistical calculations were done using SPSS software (Version 21.0.0.0, IBM Deutschland GmbH). In addition to descriptive statistics and calculation of correlation coefficients, the Shapiro–Wilk test was used to test data on normal distribution, the Mauchly test for variance

Table 2 Volunteers: respiration-dependent flow rates related to the percentage deviation from the mean blood flow

	n	End-expiration (%)	Inspiration (%)	End-inspiration (%)	Expiration (%)	*P*-value
Normal breathing[a]						
AAo	31	5.6 ± 3.0	0.04 ± 3.4	−5.8 ± 3.5	−0.7 ± 3.5	<0.05
SVC	33	4.3 ± 12.8	10.5 ± 14.1	−1.9 ± 18.7	−11.6 ± 13.5	<0.05
IVC	10	5.2 ± 16.3	22.5 ± 12.1	−5.9 ± 21.1	−13.2 ± 14.1	<0.05
Forced breathing[a]						
AAo	12	10.4 ± 5.5	−0.8 ± 4.0	−7.4 ± 6.5	2.5 ± 2.6	<0.05
SVC	12	−6.5 ± 31.1	40.0 ± 30.3	9.2 ± 18.1	−30.0 ± 19.2	<0.05
IVC	9	20.6 ± 40.6	16.5 ± 23.6	−11.0 ± 28.7	−13.7 ± 21.6	n.s.

AAo, ascending aorta; SVC, superior vena cava; IVC, inferior vena cava. n.s., not statistically significant.
[a]Data represent mean ± SD.

homogeneity. In case of normal distribution, one-way analysis of variance (ANOVA) was applied to verify whether any of the four respiratory-gated means are different considering P-values <0.05 as statistically significant. The Bonferroni test was applied to identify statistically different groups. For not normally distributed data, the Friedmann test was applied whereupon differences between groups were checked with the Wilcoxon test. Intraobserver and interobserver agreement was analysed using Bland–Altman statistics.[20]

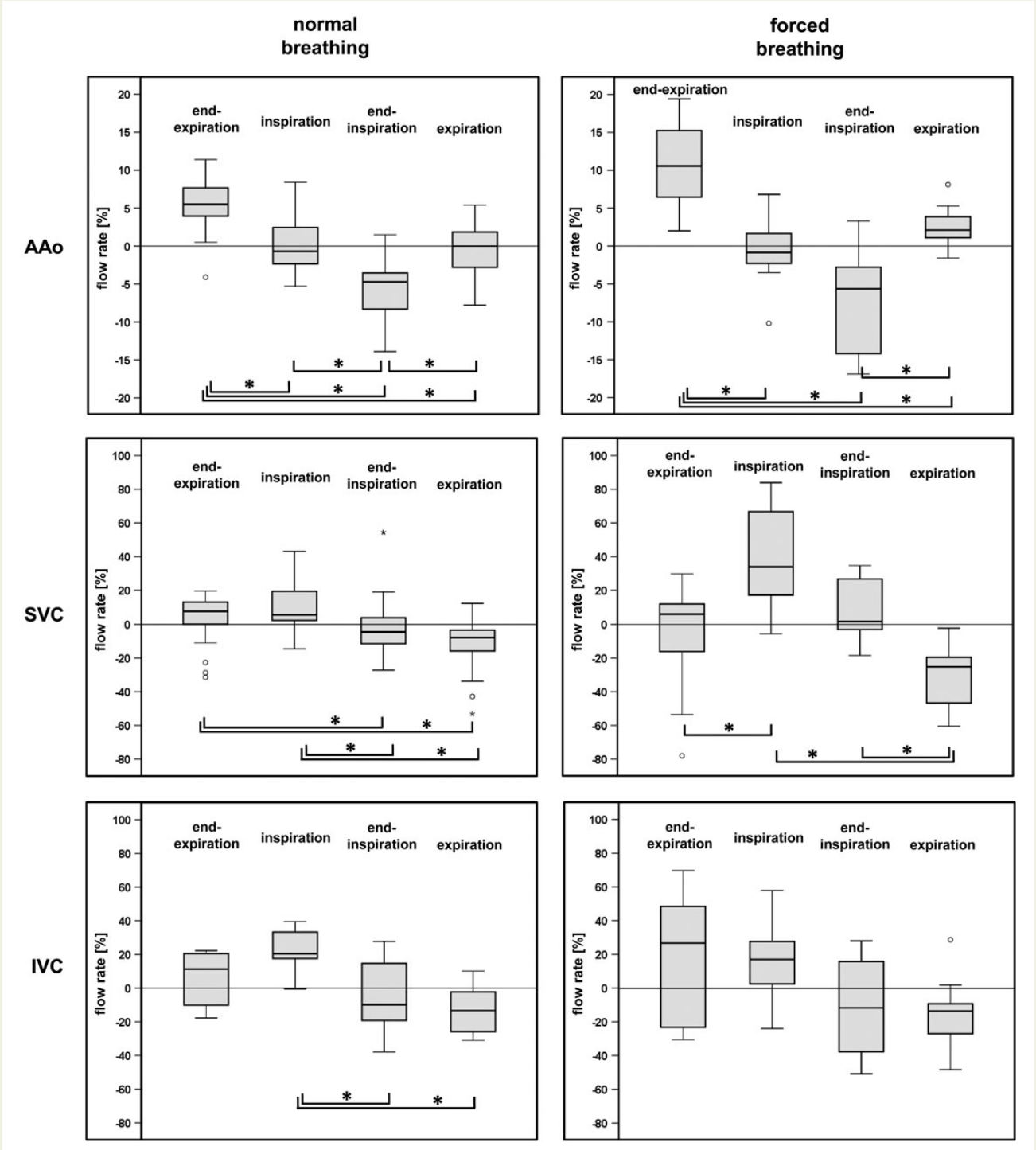

Figure 4: Respiration-dependent blood flow rates in healthy subjects. Influence of normal physiological and forced breathing on respiration-gated flow rates measured in the ascending aorta (AAo), superior vena cava (SVC), and inferior vena cava (IVC), respectively. Percentage deviation of the flow rate from the mean indexed to the body-surface. Statistical significant differences ($P < 0.05$) between the various respiratory groups are marked by an asterisk.

Results

Volunteers

All flow measurements were completed successfully with adequate image quality to perform quantitative flow analysis. One data set (AAo, 7 years, female) was excluded from the statistical evaluation due to irregular breathing of the individual.

Overall heart rate during normal breathing was 83 ± 14 and 86 ± 16 bpm during forced breathing for real-time PC-MRI. Difference was statistically not significant.

SV variability

With real-time PC-MRI SVs, fluctuations which are induced by respiration of the subject during the 12 s acquisition interval was clearly apparent. As shown in *Table 1*, the relative SV variability was around 6% for the ascending aorta and >15% for caval veins while breathing normally. If the subjects were asked to breathe in and out deeply, SVs varied >9% in AAo and >30% in veins ($P < 0.05$). To estimate the effectiveness of forced respiration, a spirometric evaluation was performed. Data were available from 10 participants. In comparison to normal respiration, on average a 3.1-fold increase of tidal volumes was observed.

Figure 3 illustrates typical flow and SV curves in a volunteer as obtained by real-time and standard conventional PC-MRI serving as reference. Note that large SV variability caused by the subject's respiration is illustrated by real-time PC-MRI but not with conventional PC-MRI due to its averaging character (data typically collected during time period between 1 and 3 min). For comparison purposes, averaged real-time PC-MRI flow and SV curves (red lines) were drawn in the figure demonstrating a similar appearance with those obtained by the reference measurement.

Respiratory influence on blood flow

To examine the impact of the individual's respiration on haemodynamics, virtual breathing-dependent SVs were generated as described earlier (*Figure 2*). As an example, the respiration-dependent aortic and upper venous SV curves were shown in the lower part of the figure. As already indicated by the considerable SV variation (*Table 1*), a strong respiratory dependency of the virtual curves was obvious.

Respiration-driven blood flow rates are summarized whereupon the given numbers correspond to the percentage deviations from mean flow (*Table 2*). Statistically significant differences between the four respiratory intervals were observed in all examined vessels.

Table 3 Intraobserver and interobserver variability: stroke volumes

	Mean	End-expiration	Inspiration	End-inspiration	Expiration
Interobserver					
Mean difference	−0.3	1.0	−3.5	−1.3	1.6
LOA	−5.8 to 5.2	−2.5 to 4.6	−15.6 to 8.6	−13.7 to 11.1	−5.7 to 8.9
r	1.000	1.000	1.000	0.998	0.999
Intraobserver					
Mean difference	3.8	3.6	4.8	3.9	3.7
LOA	0.1 to 7.6	−1.1 to 8.3	−0.1 to 9.6	−1.6 to 9.4	−0.6 to 8.1
r	0.999	0.999	0.999	0.999	0.999

Except for the correlation coefficient *r*, all values are given in percentages. LOA indicates limits-of-agreement using Bland–Altman statistics.

Table 4 Fontan patients: respiration-dependent blood flow rates related to the percentage deviation from the mean blood flow rate in the corresponding vessel

	n	End-expiration (%)	Inspiration (%)	End-inspiration (%)	Expiration (%)
Normal breathing[a]					
AAo	10	−3.6 ± 3.4	−4.1 ± 7.7	4.3 ± 9.1	7.4 ± 5.9
SVC	10	16.1 ± 19.8	22.2 ± 42.0	−20.0 ± 17.3	−12.8 ± 27.4
IVC	10	−21.9 ± 50.8	69.8 ± 39.9	54.9 ± 75.5	−78.5 ± 49.6
Forced breathing[a]					
AAo	8	−4.9 ± 5.9	−1.6 ± 6.8	0.5 ± 7.4	6.7 ± 6.4
SVC	9	25.0 ± 78.5	43.2 ± 111.1	−39.5 ± 29.5	−30.1 ± 99.4
IVC	9	−64.7 ± 62.7	125.5 ± 88.6	107.5 ± 117.7	−104.0 ± 74.7

No differentiation into patients with 'good' or 'bad' Fontan hemodynamics was performed.
[a]Data represent mean ± SD.
AAo, ascending aorta; SVC, superior vena cava; IVC, inferior vena cava.

We found that aortic flow was elevated by nearly 6% during end-expiration, whereas was reduced by the same amount during end-inspiration. The maximum blood flow in veins was detected in inspiration (10–22%) while it was minimal during expiration (−12 to −13%) whereby amplitudes were emphasized in IVC.

Regarding forced respiration increased amplitudes were observed in the AAo (end-expiration: +10%; end-inspiration: −7%, $P < 0.05$) and SVC (inspiration: +40%; expiration: −30%, $P < 0.05$) while relative blood flow remained unchanged in IVC but revealing a shifting of higher flow towards end-expiration (*Table 2*; *Figure 4*).

Generally, mean blood flow in all examined vessels did not differ between the two breathing manoeuvres ($P < 0.05$).

Intraobserver and interobserver variability

Intraobserver and interobserver variability was determined for the averaged and the four respiratory-gated SVs. Bland–Altman statistics showed high agreements (<3%) indicating neither overestimation nor underestimation with only minimal scatterings with respect to intraobserver as well as interobserver variability (standard deviation: ∼5%). Correlations were high ($r > 0.99$) in all cases (*Table 3*).

Fontan patients

Due to reduced cooperation of one patient, adequate real-time PC-MRI data were not available from the IVC (forced breathing) and SVC (normal and forced breathing). In another case of insufficient compliance, measurements had to be done under anaesthesia whereby the patients' breathing was artificially controlled (pressure controlled ventilation; normal ventilation: minute volume = 5.8 L, frequency = 17, end-expiratory carbon dioxide pressure = 35 mmHg, forced ventilation: minute volume = 7.2 L, frequency = 17, end-expiratory carbon dioxide pressure = 30 mmHg). The overall patients' heart rate was 88 ± 16 and 90 ± 14 bpm during normal and forced respiration, respectively, with no statistical significant difference.

Compared with controls, SV variability was pronounced in Fontan patients (*Table 1*). Whereas aortic SV fluctuations were only moderately elevated in both normal and forced respiration subgroups (∼11%), a doubling was observed for SVC (30–60%) and a triplication for IVC (70–120%). Simultaneously performed spirometric measurements (8 out of 10 patients) resulted in a 2.5-fold average increase of tidal volumes due to forced breathing.

For comparison with healthy subjects, the calculated respiration-dependent flow rates from Fontan patients are summarized in *Table 4*. As already observed in controls, blood flow in veins was elevated during inspiration and was considerably reduced during expiration but with increased amplitudes. This effect was most pronounced for the IVC where inspiratory flow rates exceeded the mean flow by 70%, whereas fell below the mean by −80% during expiration. Under forced breathing, such highly variable flow rates were observed for both venous vessels. Contrary to controls, highest aortic blood flow was prematurely detected during expiration in both breathing scenarios.

Regarding ΔCI_{max} comparable values of about 0.5 L/min/m^2 were found for aorta and SVC in patients and controls but were substantially elevated in the patient's IVC (3.02 ± 1.34 vs. 1.35 ± 0.51 L/min/m^2 in controls, *Table 5*). Whereas forced breathing doubled ΔCI_{max} in SVC only a weak increase was obvious in the IVC in both study groups.

In general, mean blood flow in all examined vessels in Fontan patients did not differ between the two breathing manoeuvres ($P < 0.05$).

Discussion

The study was initiated to investigate the influence of the subject's breathing patterns on blood flow in large vessels. This was achieved by applying real-time PC-MRI to measure flow in a sub-second range and by relating this information to four different respiration intervals (*Figure 2*). To our knowledge, this was the first time that virtually generated respiratory-gated SVs were created to address such dependencies in healthy subjects as well as in patients with total cavo-pulmonary connections where the patient's respiration is known to be one main factor for maintenance of blood circulation.[17,18,21]

Table 5 Mean blood flow and respiratory-dependent virtually created flow rates indexed on body surface

	AAo (L/min/m^2)	IVC (L/min/m^2)	SVC (L/min/m^2)
Healthy subjects			
Normal breathing			
Mean	4.08 ± 0.68	2.71 ± 0.46	1.57 ± 0.53
End-expiration	4.30 ± 0.68	2.85 ± 0.63	1.66 ± 0.62
Inspiration	4.09 ± 0.76	3.35 ± 0.75	1.74 ± 0.68
End-inspiration	3.85 ± 0.70	2.54 ± 0.72	1.53 ± 0.55
Expiration	4.05 ± 0.71	2.33 ± 0.40	1.39 ± 0.50
ΔCI^a_{max}	0.49 ± 0.17	1.35 ± 0.51	0.53 ± 0.31
Forced breathing			
Mean	3.93 ± 0.60	2.56 ± 0.47	1.50 ± 0.63
End-expiration	4.33 ± 0.62	2.99 ± 0.86	1.45 ± 0.84
Inspiration	3.91 ± 0.67	3.05 ± 0.98	2.09 ± 0.88
End-inspiration	3.64 ± 0.60	2.30 ± 0.93	1.65 ± 0.74
Expiration	4.04 ± 0.68	2.16 ± 0.45	1.03 ± 0.49
ΔCI^a_{max}	0.73 ± 0.35	1.93 ± 0.61	1.18 ± 0.72
Patients			
Normal breathing			
Mean	2.81 ± 0.41	1.78 ± 0.52	0.88 ± 0.44
End-expiration	2.70 ± 0.37	1.37 ± 1.04	1.05 ± 0.55
Inspiration	2.69 ± 0.43	3.08 ± 1.06	1.01 ± 0.52
End-inspiration	2.94 ± 0.59	2.80 ± 1.26	0.72 ± 0.43
Expiration	3.02 ± 0.48	0.40 ± 0.81	0.82 ± 0.48
ΔCI^a_{max}	0.52 ± 0.30	3.02 ± 1.34	0.50 ± 0.19
Forced breathing			
Mean	2.89 ± 0.59	1.57 ± 0.54	0.91 ± 0.45
End-expiration	2.75 ± 0.62	0.57 ± 0.91	1.19 ± 0.66
Inspiration	2.84 ± 0.58	3.45 ± 1.24	1.12 ± 0.61
End-inspiration	2.91 ± 0.64	3.21 ± 1.47	0.59 ± 0.45
Expiration	3.09 ± 0.67	0.06 ± 0.97	0.83 ± 0.74
ΔCI^a_{max}	0.47 ± 0.21	3.68 ± 1.74	1.00 ± 0.57

AAo, ascending aorta; SVC, superior vena cava; IVC, inferior vena cava.
[a]Maximum respiratory-related indexed cardiac output difference.

Table 6 Fontan patient characteristics

Number		Normal					Forced					Risk factor[a]	Fontan haemodynamics
		exp	In	insp	out	ΔCI_{max}	exp	in	insp	out	ΔCI_{max}		
Pt1	IVC	18.5	40.4	36.6	10.7	2.28	2.8	48.8	30.7	5.3	3.50	6	Bad
	SVC	16.4	15.3	11.5	15.6	0.38	20.1	18.4	11.8	19.1	0.64		
Pt2	IVC	16.2	62.0	83.9	−18.7	3.94	−11.7	106.5	113.8	−24.7	6.09	3	Good
	SVC	32.4	18.4	14.0	20.0	0.68	34.8	10.0	0.1	17.3	1.43		
Pt3	IVC	27.8	42.2	50.4	16.2	2.22	14.1	59.9	58.6	12.7	2.92	0	Good
	SVC	30.5	30.6	26.1	20.1	0.68	25.1	35.3	17.4	9.5	1.66		
Pt4	IVC	−2.5	35.8	51.5	−5.7	5.09	−5.7	32.7	42.7	−2.2	4.84	4	Moderate
	SVC	20.2	20.4	11.0	17.9	0.81	24.5	18.5	13.6	23.0	0.95		
Pt5[b]	IVC	15.5	10.5	2.5	8.6	0.74	16.9	11.1	1.0	8.0	0.94	4	Moderate
	SVC	15.3	11.2	10.1	14.3	0.29	13.1	9.0	7.3	12.1	0.35		
Pt6	IVC	36.7	67.4	60.1	22.4	2.07	46.0	53.1	47.9	24.5	1.35	7	Bad
	SVC	4.5	12.4	4.5	1.8	0.49	−3.9	27.8	5.7	−12.2	1.95		
Pt7	IVC	24.8	51.0	48.8	16.3	2.40	22.2	67.0	52.3	15.6	3.49	6	Bad
	SVC	18.8	19.2	14.9	17.1	0.29	20.2	17.3	14.4	19.0	0.39		
Pt8	IVC	24.7	76.7	69.1	9.1	3.37	10.1	85.9	84.6	−7.1	4.67	1	Good
	SVC	17.5	12.7	8.4	14.9	0.47	26.4	11.4	4.7	18.6	1.04		
Pt9	IVC	20.1	95.9	79.4	−21.6	4.83	−0.7	83.7	81.2	−37.6	5.31	4	Moderate
	SVC	15.3	12.3	7.7	9.4	0.30	18.0	17.2	5.0	7.6	0.57		
Pt10	IVC	49.9	58.8	15.5	15.7	3.26	–	–	–	–	–	4	Moderate
	SVC	–	–	–	–	–	–	–	–	–	–		

Stroke volumes (in millilitre) and maximum respiratory-related indexed cardiac output differences (ΔCI_{max} in L/min/m^2) as assessed by real-time PC-MRI under normal and forced breathing conditions.
exp, end-expiration; in, inspiration; insp, end-inspiration; out, expiration; ΔCI_{max}, maximum respiratory-related indexed cardiac output difference.
[a]Risk factor as defined in the methods.
[b]Examination of the patient in anaesthesia.

The increased SV variation found in venous vessels (*Table 1*, *Figures 3* and *5*) could be explained by changes in intrathoracic pressure considerably influencing the systemic venous return.[22,23] These fluctuations were enhanced (>30%) if the subjects were asked to perform forced breathing manoeuvres during data acquisition.

Regarding Fontan patients pronounced SV variability was detected. This could be related to the fact that in such patients venous blood flow is more respiratory-dependent which is based on direct interaction of the pulmonary vascular bed with the systemic venous return which takes place immediately via the pulmonary system while bypassing a morphological right heart.[16]

Respiratory-related maximal and minimal flow rates

Aortic flow in healthy subjects (*Table 2*, *Figure 4*) was highest in end-expiration and was lowest in end-inspiration. Some other researchers found higher SVs during expiration compared with inspiration but dividing the respiration curve only in two halves.[11,18] In contrast, maximal blood flow in both caval veins was observed during inspiration whereas was minimal during expiration. A similar behaviour was observed by Hjordal *et al.*[18] in the IVC but not in the SVC with unclear nature although theoretically expected in a comparable study when testing the effects of exercise and respiration on blood flow. As outlined in *Table 2*, summarizing of the two respiration gates 'inspiration' and 'end-inspiration' as well as 'expiration' and 'end-expiration' to one single phase in analogy with their study will lead to some kind of compensatory effect due to the opposite signs of the calculated flow rates. This was valid for both veins in this study demonstrating the need for virtually created SVs assigned to multiple respiratory phases to avoid averaging of flow information. Furthermore, in a recent study by Claessen *et al.*[24] a non-negligible cardiorespiratory interaction on ventricular volumes was clearly demonstrated whereupon right ventricular (RV) volumes were significantly increased during inspiration in comparison to those obtained in expiration and thus confirming the elevated blood flow in the caval veins during inspiration found in the current study since the sum of IVC and SVC flow is a surrogate for RV SV in healthy subjects. The moderate aortic blood flow during inspiration (and expiration) further explains the minor cardiorespiratory effect on LV SVs observed in the same study.

As already previously mentioned the negative intrathoracic pressure is responsible for increased inspiratory venous flow. On the other hand, simultaneously, blood pooling in the pulmonary vascular bed coupled with diminished pulmonary venous backflow into the left heart occurs.[11,25] This results in a delayed arrival of the bulk flow in the ascending aorta leading to increased left-ventricular SVs during end-expiration. Due to the aortic elasticity fluctuations in blood pressure produced by heart action[26] as well as to a minor extend the changing intrathoracic pressures are damped leading to markedly less pronounced respiratory dependency of the aortic SVs. The enhanced respiratory-induced fluctuation of the aortic SVs in Fontan patients in relation to healthy subjects (10.8 vs. 6.1%) may also reflect a capacitance function of the right ventricle in healthy subjects which possibly acts as a buffer in order to keep the

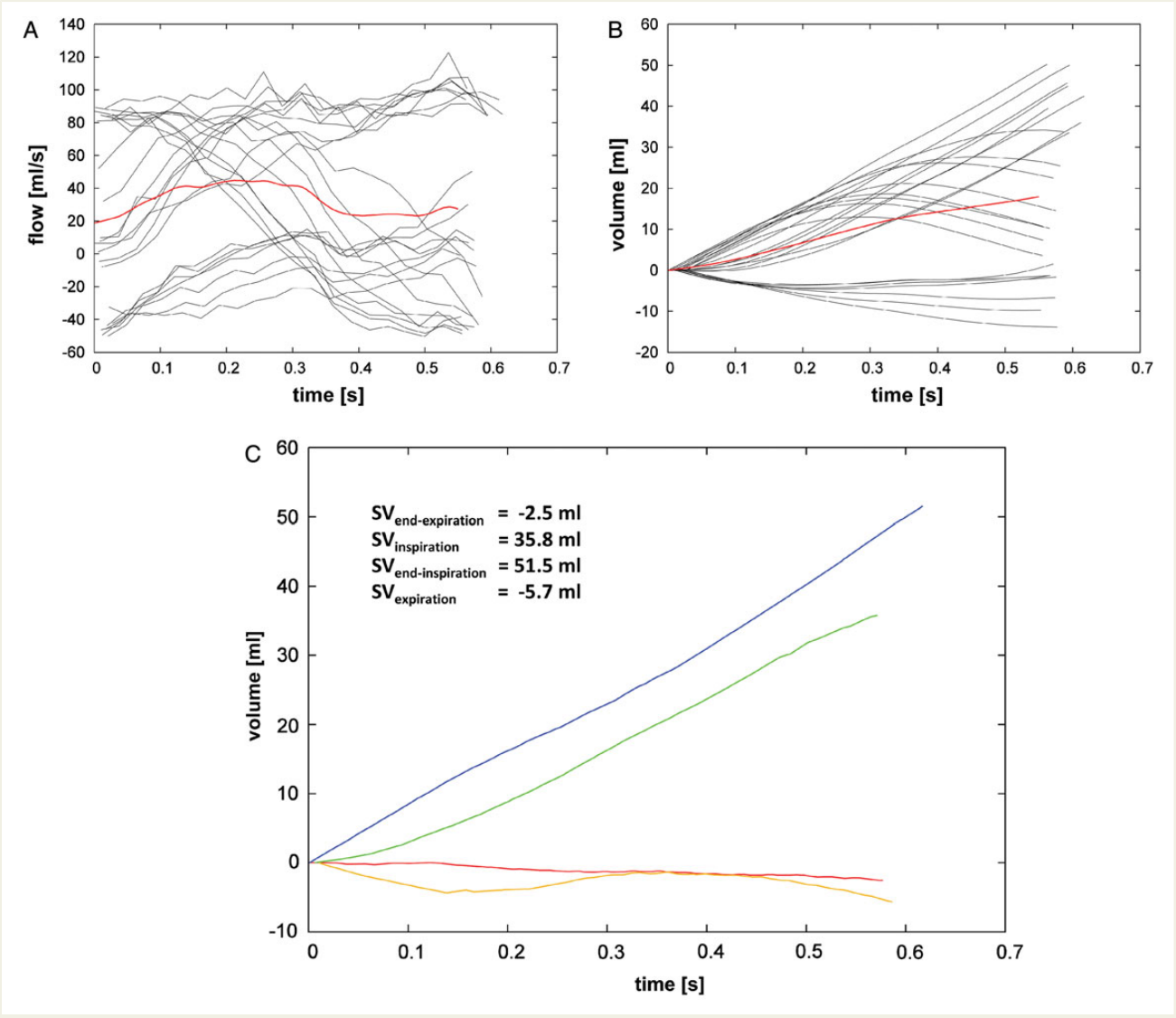

Figure 5: Fontan patient: respiration-dependent virtual SV curves. Flow rate (*A*) and SV curves (*B*) from an 11.1-year-old male Fontan patient (Pt4) obtained by real-time PC-MRI under normal breathing demonstrating the widespread physiological but systematic variation of the different heart cycles. (*C*) Computation of virtual SV curves reveals a strong blood flow towards the lungs in end-inspiration and inspiration, whereas a weak retrograde flow was detected in end-expiration and during expiration.

left-ventricular output relatively constant but which does not exist in Fontan patients with a univentricular heart.[24]

Generally, the averaged ΔCI_{max} in AAo and SVC were lower compared with those found in the IVC in healthy participants as well as in Fontan patients [~0.5 vs. 1.35 L/min/m^2 (IVC, controls), respectively, 3.0 L/min/m^2 (IVC, patients)] indicating an emphasized impact of the ventilator system on IVC blood flow variability under normal breathing (*Table 5*). It is noteworthy that forced breathing induced a doubling of ΔCI_{max} in the SVC but to a considerably lesser extent regarding the IVC (~20–40%) in both study groups. Furthermore, this study demonstrates that heart rate variations which theoretically have a significant impact on SVs were not responsible in this case because heart rates did not significantly differ between the two breathing manoeuvres neither in controls nor in the patient group.[15] In this context, it should also be mentioned that an additional skeletal muscle pump (peripheral pump) activation by introducing lower-limb exercise in Fontan patients results in a profound increase in IVC flow and to a lesser extend in SVC flow but which is mainly in consequence of an elevated heart rate.[18,27] In contrast, in our study neither mean IVC flow nor mean SVC flow were considerably changed (P = n.s.; see *Table 5*) because of restriction of the blood flow to the ventilator system alone. This observation was also confirmed by Shafer *et al.*[28] examining the relative contributions of the muscle and ventilator pumps to SVs in Fontan patients. They found an increase in the cardiac index by activating the muscle pump [change between rest and zero-resistance (0W) cycling] whereas

adding the ventilator pump by isocapnic hyperpnoea cardiac index remained unchanged. The authors assume that Fontan patients operate near their limit of contractility and that the higher blood flow induced by negative intrathoracic pressure during inspiration does not improve biomechanical coupling.

Characterization of Fontan patients

As the number of Fontan patients was limited, no statistical workup was yet performed to examine the changes in respiratory-driven flow rates in the three subgroups. Instead, a qualitative consideration was undertaken: there is some evidence that patients with a 'good' Fontan circulation behave comparable to healthy subjects (doubling of ΔCI_{max} in SVC and moderate ΔCI_{max} increase in IVC during forced breathing) but have higher ΔCI_{max} in the IVC compared with controls (e.g. Pt3, *Table 6*).

In contrast, patients with a 'bad' Fontan circulation (e.g. Pt6) a substantial non-typical increase in ΔCI_{max} and a retrograde expiratory blood flow was observed in the SVC under forced breathing accompanied by a ΔCI_{max} reduction in the IVC. This might be related to the dilated tunnel in conjunction with a diaphragmatic paresis leading to a pronounced blood supply/compensation from the SVC territory including accessory venous blood flow from the azygos vein to respond on the additional physiological demand caused by intensive respiration. As already assumed by Hsia *et al.*,[17] disturbances to the ventilator system as induced by, e.g. diaphragmatic paresis in particular hepatic venous blood flow, which substantially contributes to the total inferior venous return, is diminished in such cases leading to a detrimental effect on Fontan haemodynamics.

Furthermore, the negative influence of positive pressure ventilation on pulmonary blood flow by using anaesthesia could be observed (see Pt5, *Table 6*). Although haemodynamics was classified as 'moderate', the amount of blood flow as well as respiratory variations were diminished. It is generally known that spontaneous breathing represents the driving force for forward flow in such patients.[29] Thus, it must be assumed that the diagnostic assessment of the quality of Fontan haemodynamics is possibly not reliable if carried out under anaesthesia.

Generally, as a consequence of operative surgery, highest aortic blood flow in Fontan patients was prematurely detected in expiration. This may be related to the shorter vascular travel length (bypassing of the right heart) leading to an earlier arrival of the bulk flow at the measuring position.

Summing up there are three important factors to be concentrated on in Fontan patients: the amount of blood flow and its amplitude during respiration, the dynamics of these parameters under forced respiration, and the distinction between SVC/IVC flow may help to understand the haemodynamic consequences of tunnel aneurysms, stenotic pulmonary vessels, or massive collateral flow. This is very important because relevant pressure gradients are often difficult to detect in the venous system using invasive measurements such as cardiac catheterization.

Limitations

To inspect the extent of forced breathing during real-time PC-MRI spirometric measurements were performed simultaneously. This is an important issue since it can be expected that the amount of tidal volume changes has a direct effect on respiratory-dependent SVs and thus on the statistical evaluation. Although individual tidal volume variations were observed in this study up to date no adjustments were done.

Impairment of haemodynamics in Fontan patients may be more pronounced under exercise, we preferred to investigate the influence of the ventilatory pump alone in order to find out if this method is sensitive enough to avoid artefacts due to exercise. This could be advantageous in less cooperative patients.

Breathing in supine position may not entirely mirror haemodynamics during daily activities.

Conclusions

Real-time PC-MRI allows flow data acquisition <30 ms without any need for electrocardiographic triggering and breath-holding known to be responsible for inadequate diagnostic flow information based on respiratory-related physiological changes. The non-averaging character of real-time PC-MRI enables monitoring and studying of short-term effects such as respiratory-induced SV variations. The diagnostic potential of this method could be demonstrated in Fontan patients where respiration is known to be a crucial factor for the maintenance of blood circulation. It is expected that this technique allows evaluation of the quality of Fontan haemodynamics but may also be of value in other cardiac disease like including the non-invasive diagnostic workup of patients with pulmonary hypertension or constrictive pericarditis.

Acknowledgements

We thank Andrea Kelter-Klöpping for her support in evaluating the data.

Funding

This study was part of the project Untersuchung des respiratorischen Einflusses auf Schlagvolumina in herznahen großen Gefäßen bei Patienten mit angeborenen Herzfehlern - am Beispiel von Patienten mit Fontan-Zirkulation - mittels Echtzeit Phasenkontrast-MRT sponsored by the Fördergemeinschaft Deutsche Kinderherzzentren (project Nr. W-BDO-019/2013).

Conflict of interest: none declared.

References

1. Fratz S, Chung T, Greil GF, Samyn MM, Taylor AM, Valsangiacomo Buechel ER *et al.* Guidelines and protocols for cardiovascular magnetic resonance in children and adults with congenital heart disease: SCMR expert consensus group on congenital heart disease. *J Cardiovasc Magn Reson* 2013;**15**:51.
2. Pennell D, Sechtem U, Higgins C, Manning W, Pohost G, Rademakers F *et al.* Clinical indications for cardiovascular magnetic resonance (CMR): consensus panel report. *Eur Heart J* 2004;**25**:1940–65.
3. Stadlbauer A, van der Riet W, Globits S, Crelier G, Salomonowitz E. Accelerated phase-contrast MR imaging: comparison of k-t BLAST with SENSE and Doppler ultrasound for velocity and flow measurements in the aorta. *J Magn Reson Imaging* 2009;**29**:817–24.
4. Engvall J, Sjoqvist L, Nylander E, Thuomas KA, Wranne B. Biplane transoesophageal echocardiography, transthoracic Doppler, and magnetic resonance imaging in the assessment of coarctation of the aorta. *Eur Heart J* 1995;**16**:1399–409.
5. Hulet JP, Greiser A, Mendes JK, McGann C, Treiman G, Parker DL. Highly accelerated cardiac cine phase-contrast MRI using an undersampled radial acquisition and temporally constrained reconstruction. *J Magn Reson Imaging* 2014;**39**:455–462.
6. Kim D, Dyvorne HA, Otazo R, Feng L, Sodickson DK, Lee VS. Accelerated phase-contrast cine MRI using k-t SPARSE-SENSE. *Magn Reson Med* 2012;**67**:1054–64.

7. Johansson B, Babu-Narayan SV, Kilner PJ. The effects of breath-holding on pulmonary regurgitation measured by cardiovascular magnetic resonance velocity mapping. *J Cardiovasc Magn Reson* 2009;**11**:1.
8. Baltes C, Kozerke S, Hansen MS, Pruessmann KP, Tsao J, Boesiger P. Accelerating cine phase-contrast flow measurements using k-t BLAST and k-t SENSE. *Magn Reson Med* 2005;**54**:1430–8.
9. Markl M, Kilner PJ, Ebbers T. Comprehensive 4D velocity mapping of the heart and great vessels by cardiovascular magnetic resonance. *J Cardiovasc Magn Reson* 2011;**13**:7.
10. Jones A, Steeden JA, Pruessner JC, Deanfield JE, Taylor AM, Muthurangu V. Detailed assessment of the hemodynamic response to psychosocial stress using real-time MRI. *J Magn Reson Imaging* 2011;**33**:448–54.
11. van den Hout RJ, Lamb HJ, van den Aardweg JG, Schot R, Steendijk P, van der Wall EE *et al.* Real-time MR imaging of aortic flow: influence of breathing on left ventricular stroke volume in chronic obstructive pulmonary disease. *Radiology* 2003;**229**:513–9.
12. Thavendiranathan P, Verhaert D, Walls MC, Bender JA, Rajagopalan S, Chung YC *et al.* Simultaneous right and left heart real-time, free-breathing CMR flow quantification identifies constrictive physiology. *JACC Cardiovasc Imaging* 2012;**5**:15–24.
13. Korperich H, Gieseke J, Barth P, Hoogeveen R, Esdorn H, Peterschroder A *et al.* Flow volume and shunt quantification in pediatric congenital heart disease by real-time magnetic resonance velocity mapping: a validation study. *Circulation* 2004;**109**: 1987–93.
14. Macgowan CK, Kellenberger CJ, Detsky JS, Roman K, Yoo SJ. Real-time Fourier velocity encoding: an in vivo evaluation. *J Magn Reson Imaging* 2005;**21**:297–304.
15. Rowland TW. The circulatory response to exercise: role of the peripheral pump. *Int J Sports Med* 2001;**22**:558–65.
16. de Leval MR. The Fontan circulation: a challenge to William Harvey? *Nat Clin Pract Cardiovasc Med* 2005;**2**:202–8.
17. Hsia TY, Khambadkone S, Redington AN, Migliavacca F, Deanfield JE, de Leval MR. Effects of respiration and gravity on infradiaphragmatic venous flow in normal and Fontan patients. *Circulation* 2000;**102**:III148–153.
18. Hjortdal V, Emmertsen K, Stenbog E, Frund T, Schmidt M, Kromann O *et al.* Effects of exercise and respiration on blood flow in total cavopulmonary connection: a real-time magnetic resonance flow study. *Circulation* 2003;**108**:1227–31.
19. Hoogeveen R, Leone B, van der Brink J. Real-time quantitative flow using EPI and SENSE. *Proc. Intl Soc. Mag. Reson. Med* 2001;**9**:114.
20. Bland JM, Altman DG. Statistical methods for assessing agreement between two methods of clinical measurement. *Lancet* 1986;**1**:307–10.
21. Hart C, Gabbert DD, Voges I, Jerosch-Herold M, Andrade A, Pham M *et al.* New insights in the Fontan circulation: 4-dimensional respiratory- and ECG-triggered phase contrast magnetic resonance imaging. *J Cardiovasc Magn Reson* 2013;**15**(Suppl. 1):O38.
22. Sakuma H, Kawada N, Kubo H, Nishide Y, Takano K, Kato N *et al.* Effect of breath holding on blood flow measurement using fast velocity encoded cine MRI. *Magn Reson Med* 2001;**45**:346–8.
23. Ferrigno M, Hickey DD, Liner MH, Lundgren CE. Cardiac performance in humans during breath holding. *J Appl Physiol* 1986;**60**:1871–7.
24. Claessen G, Claus P, Delcroix M, Bogaert J, La Gerche A, Heidbuchel H. Interaction between respiration and right versus left ventricular volumes at rest and during exercise: a real-time cardiac magnetic resonance study. *Am J Physiol Heart Circ Physiol* 2014;**306**:H816–824.
25. Riggs TW, Snider AR. Respiratory influence on right and left ventricular diastolic function in normal children. *Am J Cardiol* 1989;**63**:858–61.
26. Belz GG. Elastic properties and of the human aorta windkessel function. *Cardiovasc Drugs Therapy* 1995;**9**:73–83.
27. Pedersen EM, Stenbog EV, Frund T, Houlind K, Kromann O, Sorensen KE *et al.* Flow during exercise in the total cavopulmonary connection measured by magnetic resonance velocity mapping. *Heart* 2002;**87**:554–8.
28. Shafer KM, Garcia JA, Babb TG, Fixler DE, Ayers CR, Levine BD. The importance of the muscle and ventilatory blood pumps during exercise in patients without a subpulmonary ventricle (Fontan operation). *J Am Coll Cardiol* 2012;**60**:2115–21.
29. Penny DJ, Redington AN. Doppler echocardiographic evaluation of pulmonary blood flow after the Fontan operation: the role of the lungs. *Br Heart J* 1991;**66**: 372–4.